Numerical simulation of a supercell storm over Camagüey, Cuba.

Daniel Martínez[a]*, Diana R. Pozo[a], Arnoldo Bezanilla[a], Sadiel Novo[a], Alberto García[b]

[a] Instituto de Meteorología, Apdo. 17032, La Habana 17, Cuba

[b] Centro de Investigaciones y Estudios Avanzados. Avenida del IPN 2508, México D.F.

* Corresponding author: Tel: (537) 8813411, ext. 266, e. mail: dan@met.inf.cu)

ABSTRACT

A numerical simulation is presented of the development of a supercell storm, which occurred near Nuevitas, in the Camagüey province, Cuba, on July 21, 2001. Camagüey station sounding data of 1800 GMT were used as environment for the simulation. This sounding had a high CAPE value, low wind speed with clockwise turning of the hodograph at low levels, and almost unidirectional shear in the middle troposphere. For the simulations, the three-dimensional, non-hydrostatic and compressible numerical model ARPS (Advanced regional Prediction System), of the Oklahoma University was used. Terrain and land use were included in the model. The initial state of the system was given by an ellipsoidal initial perturbation in potential temperature, located in the zone where the real storm was initially observed. A supercell storm is obtained from the simulation, which splits in two, generating two cells, which drift to the left and to the right from the general movement of the system. The greater development and lifetime of the right moving cell is explained by the characteristics of the wind field. The model results are compared with the storm evolution followed by radar.

Keywords: Cloud dynamics; Numerical modeling; Convective cloud; Supercell storm..

RESUMEN

Se presenta la simulación numérica del desarrollo de una tormenta de supercelda cerca de la ciudad de Nuevitas, en la provincia de Camagüey, el 21 de julo del 2001. Como ambiente para la simulación se utilizó el sondeo de las 1800 UTC para la estación de Camagüey. este sondeo exhibió un alto valor del CAPE, y poca velocidad del viento con hodógrafa de giro horario en los niveles bajos de la atmósfera, mientras que en la tropósfera media el shear fue casi unidireccional. Para las simulaciones se utilizó el modelo numérico tridimensional no hidrostático y compressible ARPS (Advanced regional Prediction System), de la Universidad de Oklahoma. En el modelo se incluyeron tanto el terreno como el uso de suelos. El estado inicial del sistema fue dado por una perturbación elipsoidal de temperatura potencial, situada en la zona donde se desarrolló la tormenta real detectada por el radar. A partir de la simulación de obtuvo una tormenta del tipo de supercelda, observándose su división en dos celdas, que se desplazaron hacia a izquierda y la derecha respectivamente del movimiento general del sistema. El mayor desarrollo y tiempo de vida de la celda que se mueve hacia la derecha se explica por las características del campo de viento. Los resultados del modelo se comparan con la evolución del sistema observada con ayuda del radar.

Palabras clave; Modelo numérico, nube, supercelda

1. Introduction

Supercell storm splitting has been a main research topic for numerical modelers, since 3-D models reached the ability to simulate this phenomenon. The first important results in this direction were obtained by Klemp and Wilhelmson (1978, a,b), who concluded that, in presence of a unidirectional vertical wind shear, two secondary storms form, one drifting to the right and the other to the left of the center of the system, known as the right moving and the left moving storm (SR and SL). These storms are approximately symmetrical, except for the influence of the Coriolis force, but if the shear vector turns with height in a preferential sense, then one of the cells is favored and the other is inhibited. In the most frequently observed cases of a clockwise turning hodograph, the right moving cell prevailed Later, Weisman and Klemp, (1984) showed that, for a fixed form of the hodograph, the type of storm developing as a result of the evolution of the right moving and left moving cells depends of the absolute value of the wind shear at low levels. Recently, Grasso (2000) returned to the problem of the origin of the asymmetry in the development of the two secondary cells in the presence of a curved hodograph. He showed that, for a clockwise turning hodograph, the air influx entrained in the left moving cell of the storm originated in the cold downdraft, adding negative buoyancy to it, and contributing to its dissipation.

Recently, the Advanced Regional Prediction System (ARPS) of the Oklahoma University, was customized for tropical conditions and was applied to the investigation of the development of simple convective cells over Camagüey using a real sounding corresponding to one of the PCMAT (Koloskov et al., 1996) experimental days (Pozo et al., 2001).

In the present paper, ARPS is applied to the simulation of cloud development for the hailstorm, which developed on July 21, 2001 over the region of Nuevitas, in the NE of the Camagüey province. The objective of this paper is to show that the afternoon environmental sounding, and specially the wind profile corresponding to the day of the storm can produce this type of storm, even without considering dynamic forcing produced by sea-breeze convergence. The physical mechanism explaining the development of this storm, its splitting and the prevalence of one of the secondary cells is explained. It is intended also to corroborate the hypothesis that the storm can

be classified as a supercell from the point of view of the simulation, and compare this conclusion with the analysis of radar data.

2. Numerical simulation of the July 21, 2001 hailstorm in Nuevitas.

2.1.Description of the model. Initial and boundary conditions.

The applied model is version 4.5.1 of ARPS (Xue, 1995; Xue et al., 2000, 2001). It is a mesoscale, three-dimensional, compressible and non-hydrostatic model.

As domain for the simulation, a 90x96 km mesh was used, with a horizontal step of 1 km, and 40 levels in the vertical, with a resolution of 0.5 km. The center of the mesh was located at nearly 45 km to the East of the Camagüey sounding station, at (21°35'N and 77°33'W, Fig. 1). The time step was 6 s for the calculation of all cloud parameters, and output was produced every 60 s. The simulation time was 3 hours. To initiate convection, an axially symmetric warm perturbation of maximum excess potential temperature of 4 K was applied. The perturbation was centered at x=50, y=37 and z=1.5 km, and its dimensions were 10x30x1.5 km. The form of the perturbation was chosen similar to that of the radar echo of the real storm in an early stage of development.

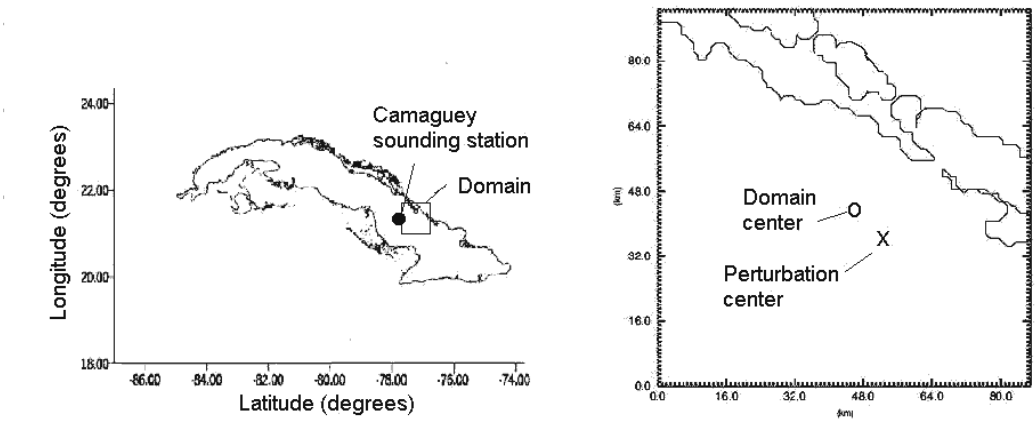

Fig 1.Location of the domain of the simulations relative to the Island of Cuba.

2.2. Meteorological situation and environment for the simulations.

The meteorological situation of July 21 was characterized by the influence of weak high pressure with surface winds from the south-southwest. The highest temperature for the Camagüey province was of 34.9 °C, and was measured in Nuevitas. The lowest temperature was also measured in Nuevitas and reached 19.4°C. In the afternoon, the sea-breeze regime was established, forming a convergence line in the northern-central part of the province.

The 1800 GMT sounding of the Camagüey station (21°25'N and 77°10'W), used as environment for the simulations (Fig 2A) exhibits a deep moist layer, a well mixed sub-cloud layer and high convective available potential temperature (CAPE), of 3351 J/kg. The low level wind is relatively weak, with variable direction, from the W-SW at low levels, but turning preferentially clockwise until the level of 10 km, which the base of a jet from the NE, which extends to the 16 km level (fig. 2B). Regarding the wind profile, three different layers can be identified in the troposphere: a low shear layer from the surface to 7 km, and a higher shear layer with wind speed increasing with height, from 7 to 12 km, and a higher shear layer with wind speed decreasing with height from 12 to 16 km.

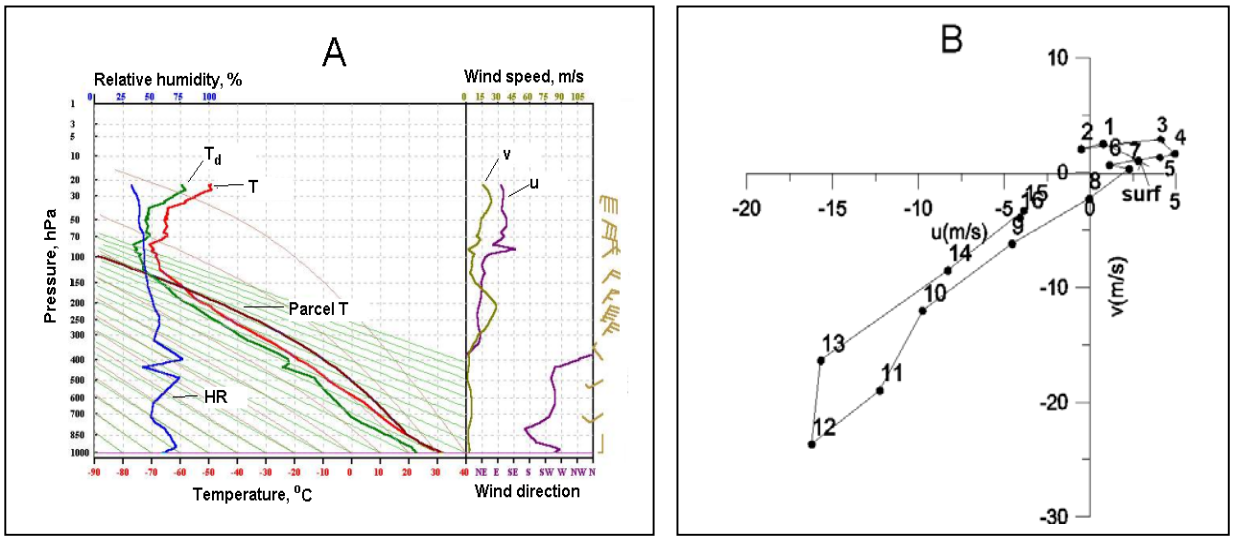

Fig 2.: A. Camaguey station 1800 GMT sounding for 7/21/2001, plotted as a Stuve diagram (left). Wind component profiles (right) B. Camaguey station 1800 GMT hodograph for 7/21/2001

2.3. Results and discussion of the simulation.

Three hours of storm life were simulated. Every 10 minutes of simulation, graphical output was obtained to analyze the evolution of the storm. To monitor significant events in cloud life, extreme values of cloud variables and their coordinates were output in text form every minute.

The first cell was initiated at 11 min. of simulation, in the coordinates of the initial perturbation. At that time, the only existing hydrometeor was cloud water q_c, with a maximum value of 0.1 g/kg. At 15 minutes it had reached 1 g/kg. At 19 minutes, rainwater q_r reaches 0.2 g/kg, which increases rapidly due to the autoconversión process. At 23 min, the rainwater content reaches 4 g/kg., the cloud top is higher than 6 km, and cloud ice content already exists. Fig 3 contains vertical cross sections of cloud water and rainwater at 30 min and 50 min. of simulation for the YZ plane. As can be observed, at 30 min. q_c reaches more than 5 g/kg (its maximum value reaches 9.4 g/kg). The higher values of q_c are located at the peripheral zone of the updraft, while the higher values of q_r (> 10 g/kg) are at its center, and a small fraction of rainfall is reaching the ground. . These high rainwater content values have originated from previous cloud water that has already evolved, because of the autoconversion process. Another fraction of the original cloud water has evolved into ice and hail at the higher levels of the cloud (Fig3B). Hail water content is already very high at this relatively early stage of cloud life, and has been able to fall through the central part of the updraft, having its maximum (> 20 g/kg) in the lower part of the cloud. Part of the hail is located lower than the 0 °C isotherm, so it contributes to rain formation by melting. At 50 min. (Fig 3C, and D), two towers have developed from the original storm, at its southern and northern sides, divided by a downdraft region, being the southern tower the higher. Rainfall is falling to the ground from the whole system. Hail is also reaching the ground from both cells.

Fig. 4 shows the presence of two vortex centers that have been generated by the interaction of the environmental wind shear with the updraft when the horizontal vortex tube is swept into it. The evolution of these vortices is shown at three moments of cloud life (30, 50 and 70 min.) for horizontal cross sections at heights of 4 and 9 km. At 30 min, the updraft at low levels (Fig. 4A) has two cores with vertical velocity greater than 10 m/s, next to two weak centers of vorticity (The central part of the updraft does not reach the maximum velocity at this level because of the load of

water content accumulating in this region, as can be inferred from Figs 3 and 6a). However, vertical vorticity is much greater at higher levels (Fig 4B), showing two well-structured regions of positive and negative vorticity, whose center is located in the periphery of the updraft core, reaching a vertical velocity of 42 m/s in its center. The rapid strengthening of the updraft through the middle troposphere is a consequence of the high CAPE. This can be better observed for the 6 km level (Fig. 5), where the high acceleration of the updraft produces an increase in lateral entrainment in early stages of cloud development (Figs 4A,5A). The combined effect of entrainment and of the increase in wind shear observed above the 7 km level (Figs. 1 and 2) favors the organization of the vorticity centers at higher levels.

The cyclonic and anticyclonic vortices, shown in Fig 4B are consistent with the conceptual model of a convective simple cell cloud (Houze, 1993), which coincides with the first step of a supercell development. At 50 minutes of simulation, the vortex centers at the north and south of the updraft reinforce at the 9 km level. A central downdraft region divides the updraft for all levels, generating two convective cells. This downdraft overlaps with the southern high water content zone shown in Fig. 6, produced by high rainwater and melting hail content at low levels, and by the formation of hail and snow in the upper levels. The influence of the loading of this hydrometeors seems to be the major cause of the splitting of the initial updraft, which was a gradual process, occurring progressively from the base to the top of the cloud (Fig. 6) The vertical velocity, vorticity and reflectivity patterns are consistent with the conceptual model of a supercell developed by Klemp and Wilhelmson (1978b) (Figs 4,6 (C and D)). Two pares of cyclonic and anticyclonic vortices, corresponding to the two newly generated convective cells that can be identified as the left moving and right moving storms, according to their movement direction relative to the center of the system. One the storm has split, the internal wind structure shows asymmetry in the sense that the left moving storm entrains downdraft cold air to its southern flank, blundering with the central downdraft, while the right moving storm entrains mainly environmental air into its northern flank (Figs 4C, 5B).

The analysis of the pressure perturbation (not shown) leads to the conclusion that both updraft zones nearly coincide with two pressure minima, independently of the vorticity sign. At 50 minutes, at the 4 km level, a high pressure zone exists, associated with the downdraft, persisting at 70 minutes.

Fig 3 (E a nd F) shows the structure of the southern cell (SR) in the XZ plane, passing through the maximum velocity zone. Here can be seen the formation of the anvil, consisting of cloud ice, hail and snow (only ice and hail shown). Hail content under the anvil is very small, near to 0.01 g/kg, which would be related in a real cloud with small graupel particles. This hail content melts in its way down, forming rainwater and cloud water, which partially evaporate before reaching the ground. The evaporation rate is greater the farther from the main body of the cloud, because of the interaction with drier environmental air, so that the depth of the rainwater layer increases with the x coordinate.

At 70 min., SL starts to dissipate at the 4 km level. At 9 km, the system keeps its structure, but the updraft area of SL smaller than that of SR (Figs. 4, 6 (E and F). At 80 min., both cells go on raining on the ground, but the northern cell produces no more hail. The top of SR, formed mainly by cloud ice have descended nearly 2 km, keeping the 0.1 g/kg contour as a boundary criterion, and ice water content still reaches more than 2 g/kg, while hail content reches more than 1 g/kg,. However, the top of SL have descended much more, while its ice and hail water contents don't reach 1 g/kg. (Fig. 7).

Figs. 4 and 6 show that the system is moving slowly towards the E-NE, approximately in the direction of the average wind, in the 1-7 km layer. The two cells shift slowly to the northern side (left) and the southern side (south) from the center of the system, being the southern cell (SR) the one reaching a greater development and lifetime. Fig. 8 shows the paths of the two cells and the approximate center of the system during the first 80 minutes of storm life. Afterwards, SL accelerates its dissipation, though rain and ice persist for an hour more. SR keeps in the mature stage for approximately two more hours. Afterwards, maximum updraft velocity lowers to less than 2 m/s, though rainfall keeps falling for half an hour more. At 180 min., reflectivity has become less than 20 dBz.

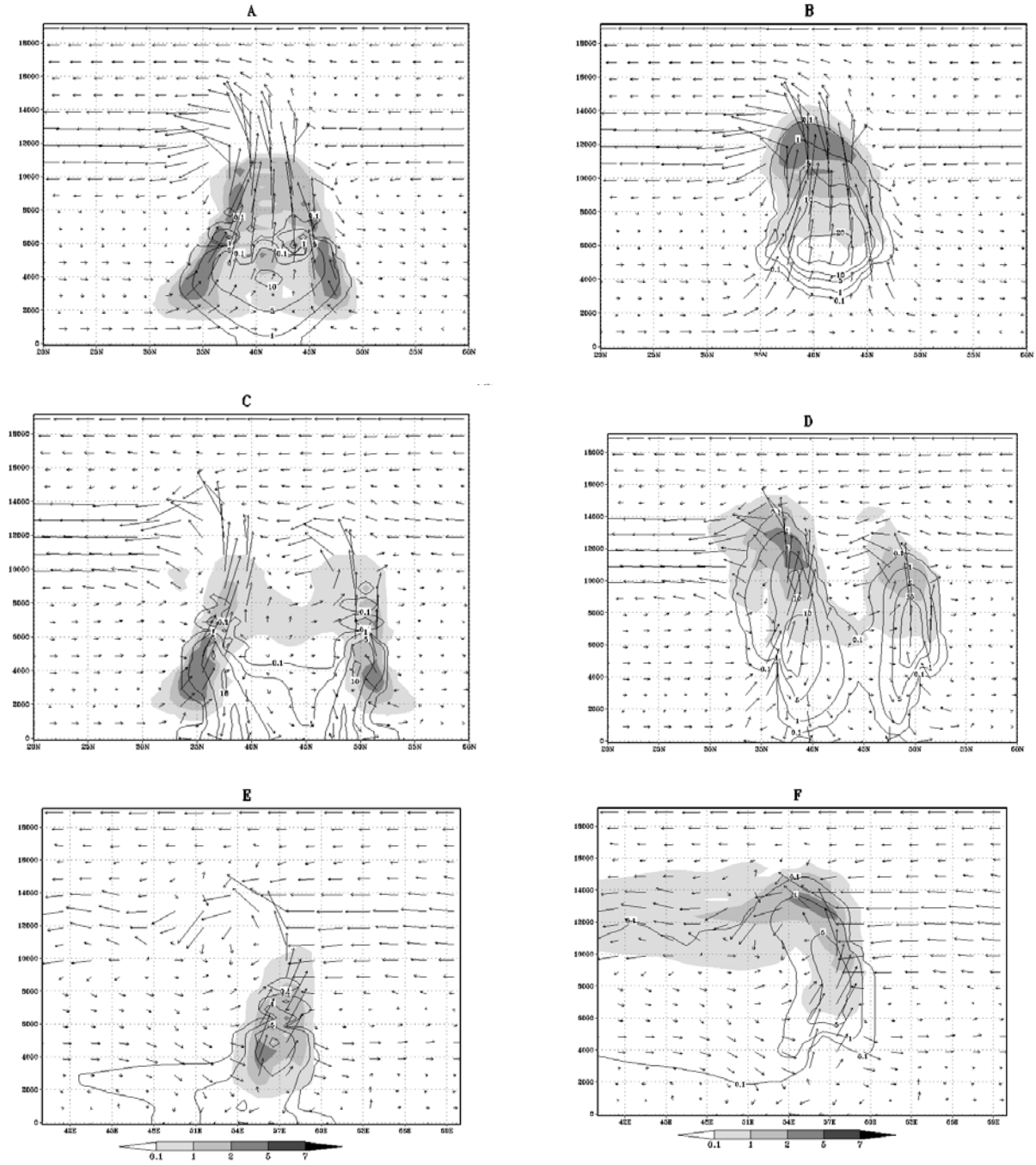

Fig 3. Vertical cross sections by the plane of maximum vertical velocity of mixing ratios for cloud water, rain water, ice and hail (g/kg). Vectors represent the projection of the three-dimensional wind vector in the plane of the figure.

A: Y-Z plane, x=53.5 km, t=30 min. Shaded: cloud water. Contour: rainwater.

B.: Y-Z plane, x=53.5 km, t=30 min. Shaded: ice water. Contour: hail.

C: Y-Z plane, x=56.5 km, t=50 min. Shaded: cloud water. Contour: rainwater.

D: Y-Z plane, x=56.5 km, t=50 min. Shaded: ice water. Contour: hail.

E: X-Z plane, y=36.5 km, t=50 min. Shaded: cloud water. Contour: rainwater.

F: X-Z plane, x=36.5 km, t=50 min. Shaded: cloud water. Contour: hail.

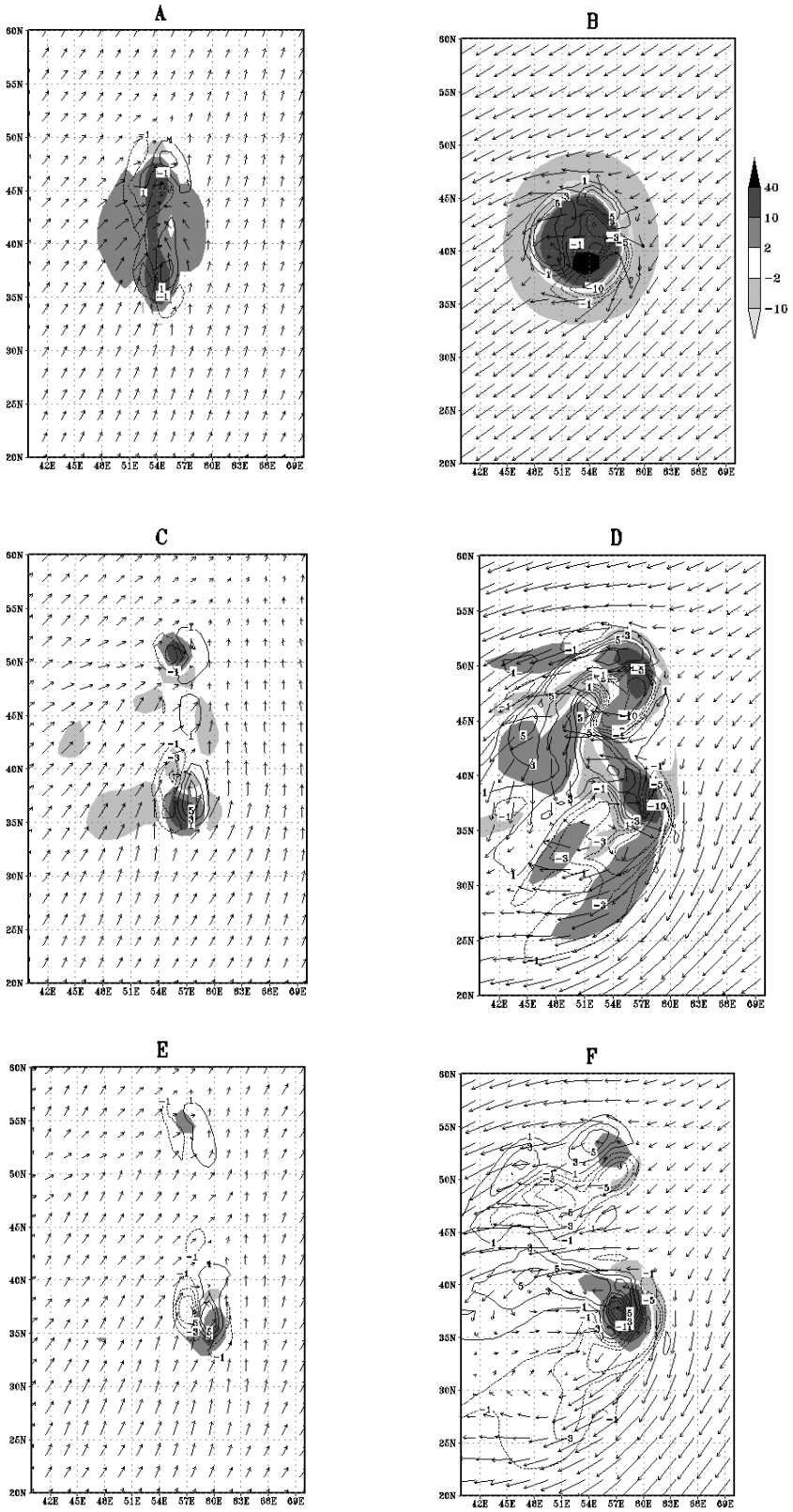

Fig 4. Horizontal cross sections of vertical velocity (m/s) and vorticity (x 10^{-3} s^{-1}).
Shaded: Vertical velocity. Contour: Vertical vorticity.
A: z = 4 km, t = 30 min. B. z= 9 km, t = 30 min.
C: z = 4 km, t = 50 min. D: z = 9 km, t = 50 min.
E: z = 4 km, t = 70 min. F: z = 9 km, t = 70 min.

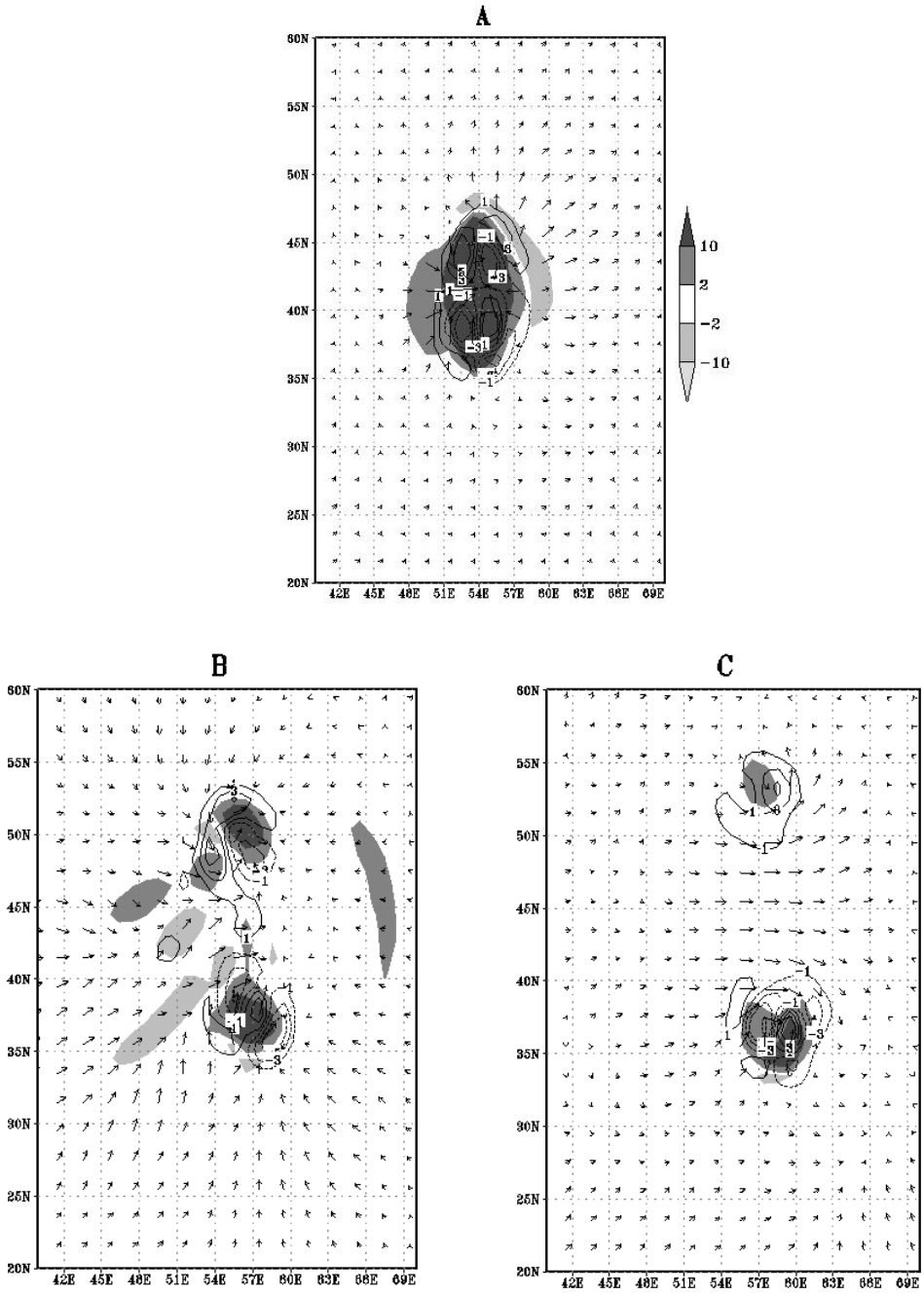

Fig 5. . Horizontal cross sections of vertical velocity (m/s) and vorticity (x 10^{-3} s^{-1}). Shaded: Vertical velocity. Contour: Vertical vorticity. z = 6 km.
A: t = 30 min., B: t = 50 min., C: t = 70 min

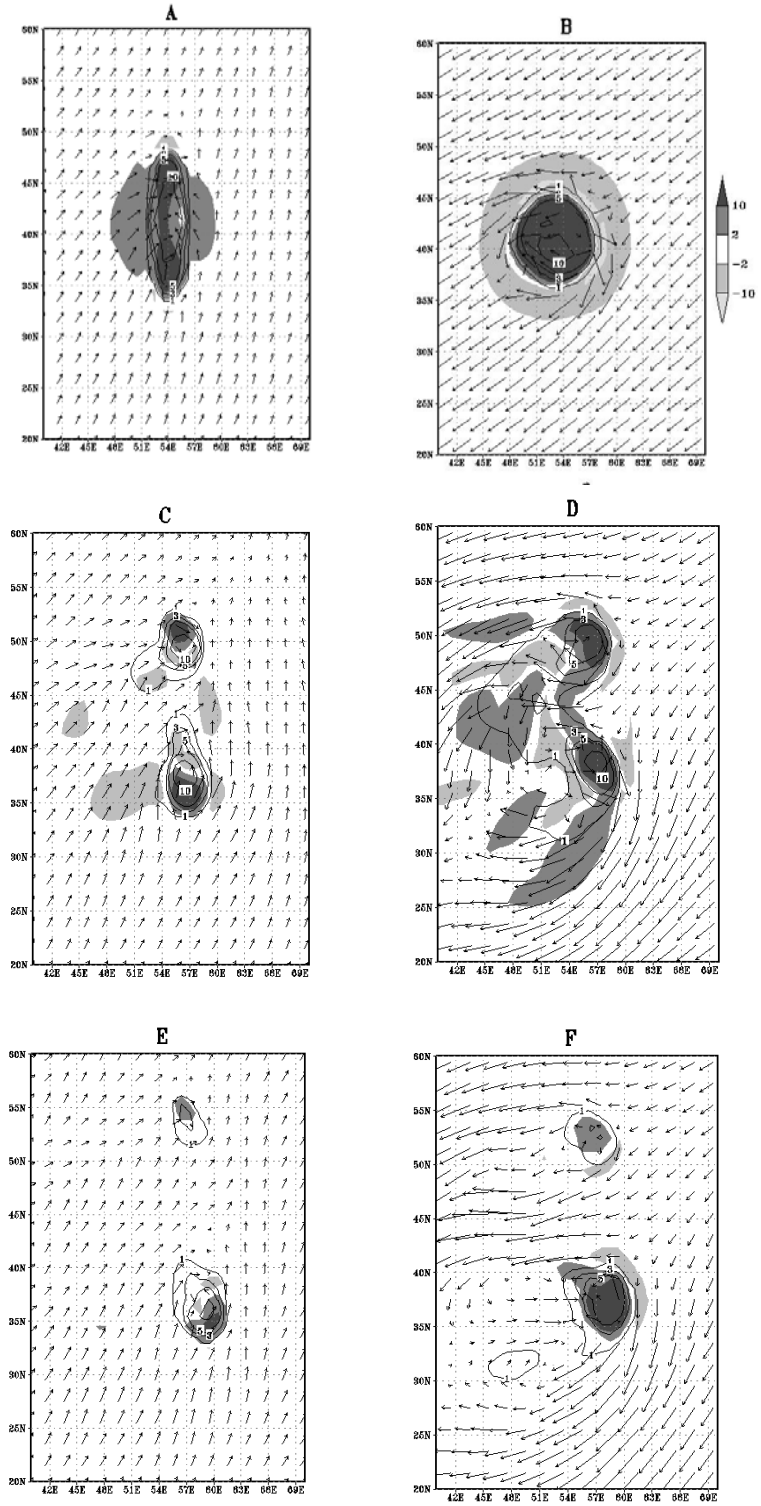

Fig 6. Horizontal cross sections of vertical velocity (m/s) and total water content (g/kg). Shaded: Vertical velocity. Contour: Total water content.
A: z = 4 km, t = 30 min. B. z= 9 km, t = 30 min.
C: z = 4 km, t = 50 min. D: z = 9 km, t = 50 min.
E: z = 4 km, t = 70 min. F: z = 9 km, t = 70 min.

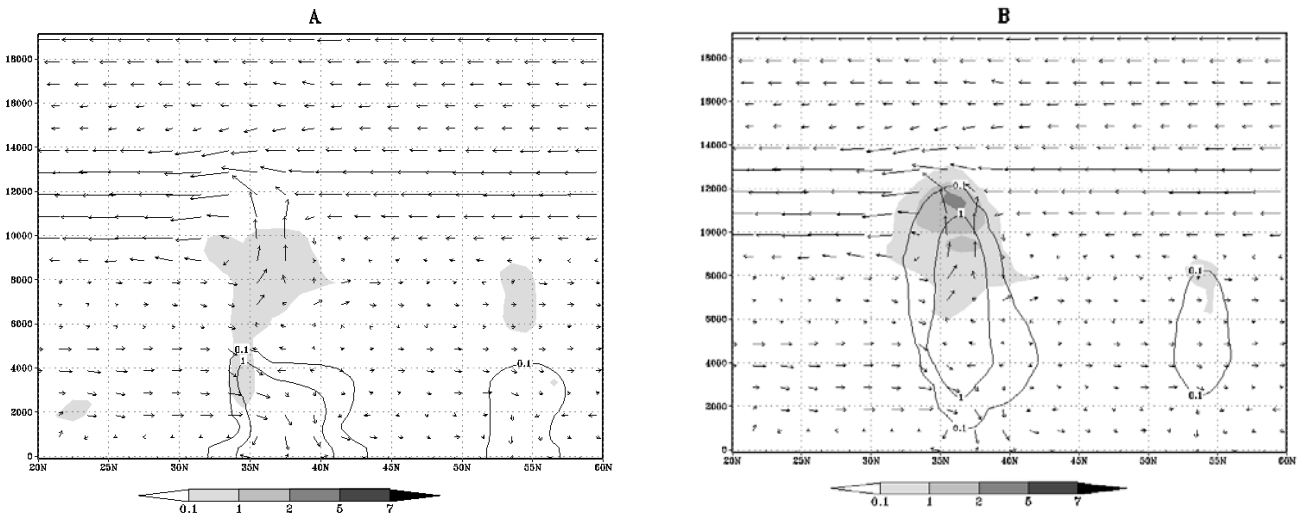

Fig 7. Vertical cross sections of mixing ratios for cloud water, rain water, ice and hail (g/kg) by the Y-Z plane crossing the point of maximum vertical velocity for the beginning of the dissipation stage of the system (t=80 min.) Vectors represent the projection of the three-dimensional wind vector in the plane of the figure. x = 59.5 km.
A. Shaded: cloud water. Contour: rainwater
B. Shaded: cloud water. Contour: hail.

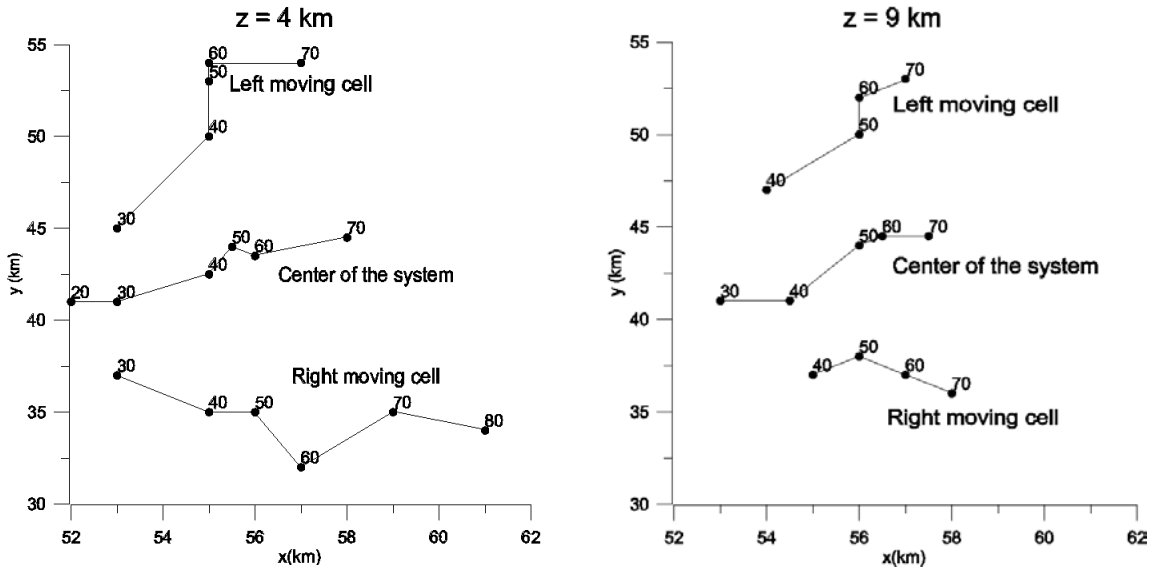

Fig 8. Trajectories of the centers of the left moving cell, the right moving cell and the center of the system. The labels indicate simulation time in minutes. (Right: z = 4km; Left: z = 9 km)

In this case, the hodograph turns clockwise with increasing height, and the more developed storm is the right moving one (SR), according with Klemp and Wilhelmson (1978 b) results. However, in the present simulation, the difference between both storms is no so great in early stages of system development after the splitting. This can be explained from the characteristics of the shear flow at low levels. In the lower 6 km the wind is relatively weak and there is preferential clockwise turning of the hodograph, but it is accompanied by significant variations in wind shear direction, so that the net effect in the difference between the vertical pressure gradients in the southern and northern flanks of the storm in its early stage of development is less than in Klemp and Wilhelmson's simulations. However, between 6 and 12 km, the increment in wind shear intensity is remarkable, while the wind shear vector direction is nearly constant, making possible the development of both cells. The final predominance of SR may be due to the inclusion of cold air, coming from the central downdraft at middle levels, as can be observed from fig 4C and 5B. This mechanism was discussed by Grasso (2000) as one of the possible causes of asymmetry in the development of split storms.

3. Radar observations.

Radar observations of the Nuevitas storm of July 21, 2001 roughly corroborate the above simulations results (Novo et al., 2003), though there are important differences which are related with the interactions of several convective systems in the area. As convective development took place in different zones of the province from the early afternoon, the system that was present at the initial simulation time was the result of previous interactions of different systems. Fig. 9 shows the evolution of the radar echoes of the system, from a threshold of 20 dBZ. At 22:35 GMT, the "original" cell is observed; showing a reflectivity maximum in its center at both levels, and corresponds to the central downdraft in the simulation. At 22:46 GMT, in the lower level the splitting process has begun, while in the upper level, a decrease in reflectivity is observed. Nine minutes later, the cores of both cells are separated in the lower level, and in the upper levels, the cells are totally separated, using the 20 dBZ threshold. Fifteen minutes later, precipitation is again observed in the lower level between the two cells. The southeastern cell has developed very fast, but I the upper level both cells appear as independent. At 23:10, the southeastern cell, which deviates gradually rightward, dominates in both levels. This is the time at which hail

was detected on the ground. At 23:30, the left cell has practically disappeared, while the right cell continues its development for an hour more.

The simulation reproduces the main features of the observations, regarding both the general evolution of the system and the range of reflectivity values, showing that the development of a supercell from a simple cell storm is a consequence of the evolution of the system in the environment given by the sounding, even if it does not meet the requirement of having large shear at low levels. This was the main objective of the simulation, and the chosen options for running the model were the simplest possible not to complicate the analysis.

However, the simulation was unable to reproduce the sizes and lifetimes of the cells resulting from the splitting of the original storm. This partial lack of coincidence is related to some limitations in the application of the model. The first is that the time of the nearest available sounding was some hours before the beginning of the storm, so that two other convective systems had developed in the province before the time chosen as “initial” (Novo et al., 2003). On the other hand, the site of the sounding was located nearly 40 km distant from the zone where the studied system developed. Another limitation of the results is the arbitrary election of the initial perturbation, considering that the real system existed before of the starting time of the simulation, and was the result of merging of preexisting systems. In a paper in preparation, the same case will be analyzed, using time-dependent boundary conditions, inserting the model into the output of a limited area model, and including dynamic information from the surface meteorological network.

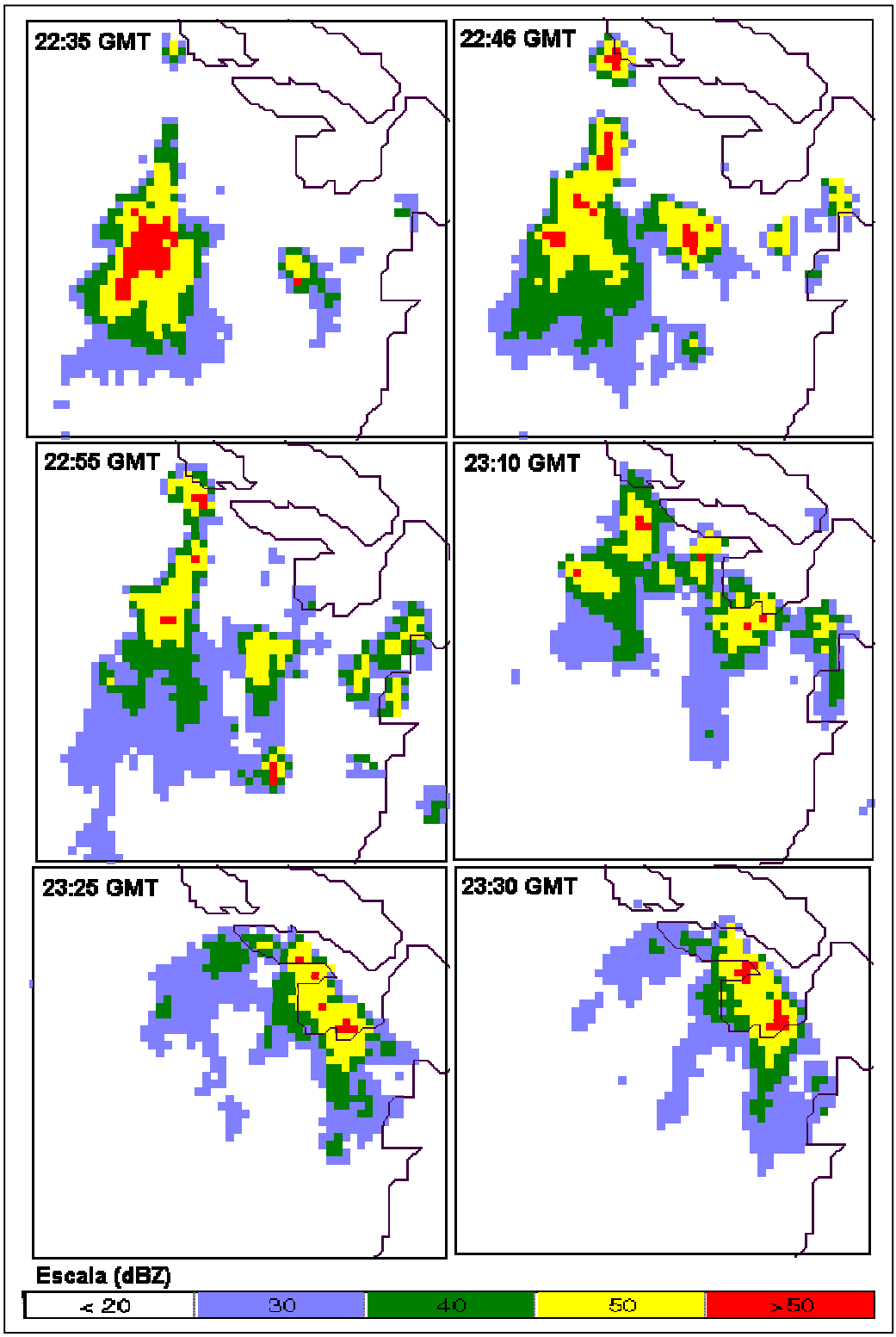

Fig 9A. Evolution of the storm radar echo field. . CAPPI of the 3-4 km layer.

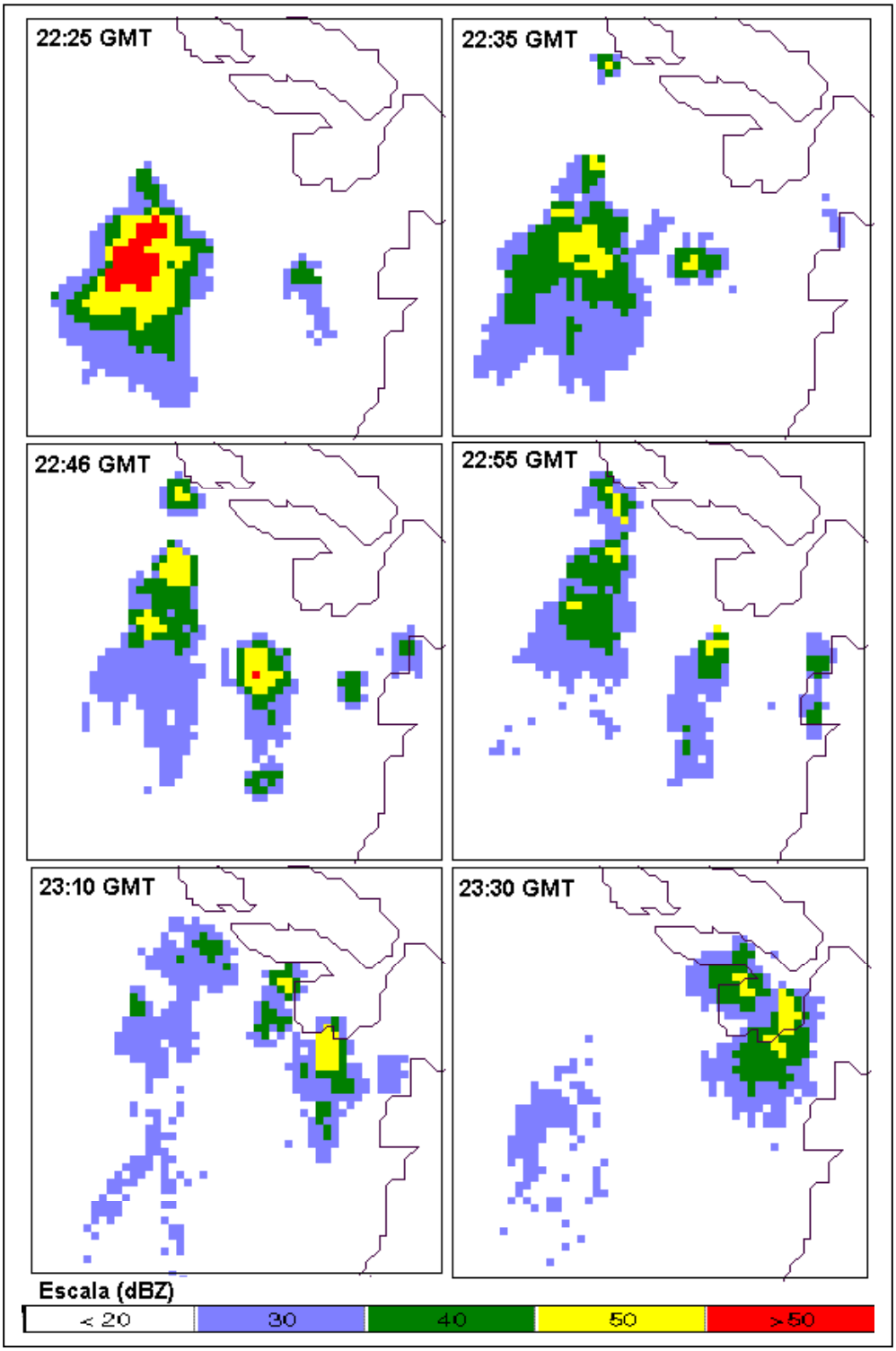

Fig 9B. Evolution of the storm radar echo field.. CAPPI of the 9-10 km layer

4. Conclusions

Numerical simulation results corroborated that the July 21, 2001 Nuevitas severe storm consisted in the right moving cell of a supercell system, generated in an environment of high instability, and a wind profile characterized by clockwise turning hodograph with low wind speeds at the lower levels and strong, and nearly unidirectional wind shear at heights from 6 to 12 km.

The structure of the simulated storm presents two secondary cells derived from an original simple cell. These cells displace to the left and right directions relative to the original storm motion, which coincides with the direction of the mean wind vector in the layer from 1 to 6 km. The cells have cyclonic and anticyclonic vortices, associated with associated with updrafts and negative pressure perturbations, but these do not manifest clearly at low levels.

The left moving and the right moving cells develop similarly in relatively early stages of storm development, but after 70 min. of simulation, the left cell begins to dissipate, while the right moving one remains stable. The probable reason for the relatively early dissipation of the left moving cell is the entrainment of cold air, generated in the central downdraft at low and middle levels, by the mechanism reported by Grasso (2000), while the right moving cell entrained environmental air, which is conditioned by the wind profile.

The simulation reproduces the main features of the observations, regarding both the general evolution of the system and the range of reflectivity values, showing that the development of a supercell from a simple cell storm is a consequence of the evolution of the system in the environment given by the sounding, even if it does not meet the requirement of having large shear at low levels.

References

Amador, E., Batista, L.M. et al., 1987. Radar investigation of summer showers in the region of the Camagüey Experimental Area. Tropicheskaya Meteorología. Trudy Tretevo Mezhdunorodnovo Simpoziuma. 539 – 545. (in Russian).

Alfonso, A., 1994. Climatología de las Tormentas Locales Severas de Cuba. Cronología. Editorial Academia. La Habana, pp 167.

Alfonso, .A. and Córdoba, L. 1987. Los mesociclones del 16 de Febrero en las

provincias habaneras. Reporte de investigación. INSMET Cuba #16, 26 pp.

Alfonso, L., Martínez, D. and Pérez, C. A., 1998. Numerical simulation of tropical convective clouds over Cuba using a one-dimensional and time-dependent cloud model. ATMOS. RES., 47-48.343-354.

Beliaev, V., Valdés, M., Martínez, D. and Petrov, V. , 1989. An airborn study of the structure of cloud bands observed over the Camagüey Experimental Area (in Russian). Trudy TsAO, 172,11-16

Bluestein, H. B., and Sohl, C. J.,1979. Some observations of a splitting severe thunderstorm . Mon. Weather Rev. 112, 2253-2269.

Browning, K. A., 1964. Airflow and precipitation trajectories within local severe storms which travel to the right of the winds J. Atmos. Sci., 21, 634-639.

Browning, K. and Foote, G. B., 1976. Airflow and hail growth in supercell storms and some implications for hail suppression. Q. J. R. Meteorol. Soc. , 102, 499-533.

Byers, H. R. and Braham, R. R., (1949). The Thunderstorm. U.S. Weather Bur., Washington D. C. 287 pp.

Clark, T. L., 1979. Numerical simulations with a three-dimensional cloud model: Lateral boundary condition experiments and multicelular storm simulations. J. Atmos. Sci, 36, 2191-2215.

Knupp and Cotton, 1982. An intense, quasi-steady thunderstorm over mountainous terrain – Part II: Doppler radar observations of the storm morphological structure. J. Atmos. Sci. 39, 343-358.

Grasso, L. D., 2000. The dissipation of a left-moving cell in a severe storm environment. Mom. Weather Rev., 128, 2797-2815.

Gamboa, F., . Aroche, R,. Boza, L, Finalé, A., 2001a. Una granizada poco común en Las Tunas, Cuba. Memorias del IX Congreso Latinoamericano e iberoamericano de Meteorología. Biblioteca Nacional de Buenos Aires Argentina. Sesión 8.C.1 N° 29.

Houze, R. A., Jr., 1993. Cloud Dynamics. . International Geophysics Series. Vol. 53., 573 pp. Academic Press.

Kessler, E., 1969. On the distribution and continuity of water substance in

atmospheric circulation. Meteorol. Monogr. 10.

Klemp, J. B, and Wilhelmson, R. B., 1978a. The simulation of three-dimensional convective storm dynamics. J. Atmos. Sci., 35, 1070–1096.

Klemp, J. B, and Wilhelmson, R. B., 1978b. Simulations of right- and left- moving storms produces through storm splitting J. Atmos. Sci., 35, 1097-1110.

Koloskov, B., Zimin, B., Beliaev, V., Seregin, Y.,Chernikov, A., Petrov, V., Valdés, M., Martínez, D.,Pérez, C. and Puente, G, (1996). Results of Experiments on Convective Precipitation Enhancement in the Camagüey Experimental Area. Cuba. Jour. Appl. Meteor., 45, 9, pp. 1524-1534.

Lin,Y. L., Farley, R. D., and Orville, H. D., 1983. Bulk parameterization of the snow field in a cloud model. J. Clim. Appl. Meteor., 22, 1065-1092.

Martínez, D., 1995. Caracterización de la turbulencia y la convección en las nubes convectivas sobre el Polígono meteorológico de Camaguey. Tesis en opción al grado de Doctor en Ciencias Físicas. Instituto de Meteorología. Ministerio de Ciencia, Tecnología y Medio Ambiente. Cuba, 128 pp.

Martínez, D., 1999. Turbulence Parameters and Vertical Drafts in Cuban Convective Clouds. Rev Bras. Meteor., , Vol. 14, No. 2

Martínez, D. and Gori, E. G., 1999. Raindrop size distributions in convective clouds over Cuba. ATMOS. RES.., 52, 221-239.

Novo, S, Martínez, D., Gamboa, F. and Aroche, R.,2003. Estructura interna de diferentes tipos de tormentas convectivas observadas sobre Camaguey, a partir de datos de radar. Publicado en estas Memorias.

Pozo, D., Martínez, D. and Chacón, M., 2001. Simulación numérica tridimensional de una celda convectiva simple en condiciones tropicales utilizando el modelo ARPS. Rev. Cub. Meteor., 8, 1, 74-82.

Rotunno, R. and Klemp, J. B., 1982. The influence of shear-induced pressure gradients on thunderstorm motion. Mon. Weather. Rev., 110, 156-171.

Rotunno, R. and Klemp, J. B., 1985. On the rotation and propagation of simulated supercell thunderstorms. J. Atmos. Sci. 42, 271-292.

Schlesinger, R. E., 1980. A three-dimensional numerical model of an isolated

thunderstorm. Part II. Dynamics of updraft splitting and mesovortex couplet evolution. J. atmos. Sci. 37, 395-420

Trípoli, G. J and Cotton, W. R., 1986. An intense quasi-steady thunderstorm over mountainous terrain. Part IV. Three dimensional numerical simulations. J. Atmos. Sci. 43, 894-912.

Weisman, M. L., and Klemp, J. B., 1982. The dependence of numerically simulated convective storms on vertical wind shear and buoyancy. Mon. Wea. Rev., 110, 504–520.

Weisman, M. L., and Klemp, J. B., 1984. The structure and classification of numerically simulated convective storms in directionally varying wind shears:. Mon. Wea. Rev., 112, 2479-2498.

Xue, M., Droegemeier, K. K., Wong, V., Shapiro, A., and Brewster, K.,1995. ARPS Version 4.0 user's guide. Center for Analysis and Prediction of Storms, Univ. of Oklahoma, 380 pp. [Available from CAPS, 100 E. Boyd St., Norman, OK 73019.]

Xue, M., Droegemeier, K.K.and Wong, V., 2000. The Advanced Regional Prediction System (ARPS) – A multi-scale nonhydrostatic atmospheric simulation and prediction model. Part I: Model dynamics and verification. Meteorol. Atmos. Phys. 75, 161-193.

Xue, M., Droegemeier, K.K., Wong, V., Shapiro, A., Brewster, K., Carr, F., Weber, D., Liu, Y. and Wang, D., 2001. The Advanced regional prediction System (ARPS) – A multi-scale nonhydrostatic atmospheric simulation and prediction model. Part II: Model physics and applications. Meteorol. Atmos. Phys. 76, 143-165.

Acknowledgments. The authors want to thank Felix Gamboa and Roberto Aroche, from the Camagüey Meteorological Center, for organizing the radar observations and part of the meteorological information. Support for this work was provided by the Cuban-Mexican CITMA-CONACyT project E120.1306 and the Cuban CITMA project 49204212. The simulations were made using the Advanced Regional Prediction System (ARPS) developed by the Center for Analysis and Prediction of Storms (CAPS), University of Oklahoma. CAPS is supported by the National Science Foundation and the Federal Aviation Administration through combined grant ATM92-20009.